UDC 544-16

Microstructure of Cold Rolled Magnesium and Magnesium Hydrides for Hydrogen Storage Applications

J. LANG[1], N. SKRYABINA[2], D. FRUCHART[3], M. DANAIE[4] and J. HUOT[1]

[1]*Chemistry and Physics Department, Université du Québec à Trois-Rivières, 3351 des Forges, Trois-Rivières, Québec, G9A 5H7 (Canada)*

[2] *Department of Physics, Perm State University, Ul. Bukireva 15, Perm 614990 (Russia)*

[3] *Institut Néel BP 166, 38042 Grenoble Cedex 9 (France)*

[4]*Department of Materials Science and Engineering, McMaster University, Hamilton, Ontario (Canada)*

E-mail: jacques.huot@uqtr.ca

Abstract

It has recently been shown that Severe Plastic Deformation (SPD), and particularly cold rolling, techniques could be used to obtain nanostructured metal hydrides with enhanced hydrogen sorption properties. Cold rolling is a particularly interesting technique because it is easily scalable to industrial level. We present here the effect of cold rolling on hydrogen storage properties of magnesium and magnesium hydride (MgH_2). Commercial magnesium and magnesium hydride were processed in a vertical cold rolling apparatus. For pure magnesium, a highly textured material was obtained after only one roll and first hydrogenation was faster than unprocessed magnesium. In the case of magnesium hydride, after only five rolling passes hydrogen sorption kinetics at 623 K were greatly enhanced without noticeable loss of capacity. The improvement in sorption kinetics is attributed due to the nanocrystalline structure and number of created defects. Investigation of the powder morphology and crystal structure indicates that cold rolling is equivalent to ball milling.

Key words: hydrogen absorbing materials, magnesium alloys, cold rolling, gas-solid reactions

INTRODUCTION

Magnesium is considered to be a good candidate for hydrogen storage technologies mainly because of its large hydrogen storage capacity (7.6 mass %), reversibility and low cost. However, magnesium hydride has to be at a temperature of at least 280 °C to be able to desorb hydrogen under a pressure of one bar. This puts high constraints on the applicability of magnesium for practical applications. Another constraint is the cost to produce and process magnesium hydride. Even if magnesium itself is relatively inexpensive, the first hydrogenation of magnesium could be very expensive because the material has to be either exposed to high hydrogen pressure at high temperature for a long time or cycled many times. In either case, the process is slow and greatly increases the production cost of magnesium hydride. Therefore, researches have been targeted to improve the hydrogenation properties of magnesium, such as appropriate alloying of magnesium [1–3], adding catalyst, and manufacturing nanocrystalline powder.

The technique of ball milling has been extensively used to synthesize and process metal hydride in order to get nanocrystalline structures and nanocomposites [6–9]. However, high energy milling may be difficult to scale up to industrial level due to capital and operational costs. Cold rolling is an attractive alternative

to ball milling because it is already used by the industry and, under specific conditions, has similar mechanical effect as ball milling. In the last few years a series of papers have shown that repeated cold rolling (CR) produces enhancement of hydrogen storage properties in metal hydride, particularly for magnesium and magnesium-based alloys [10–23].

Amongst the numerous severe plastic deformation (SPD) techniques, we report here just one technique: cold rolling. This technique was selected because it could be easily scaled up to industrial level. In this paper, we report the effect of cold rolling on the crystal structure and hydrogen storage properties of magnesium and magnesium hydride. In the case of magnesium, the main subject of investigation was the first hydrogenation, the so-called activation step. It is well known that activation of magnesium is a very slow process and has to be carried out at high temperature and pressure and/or many hydrogenation/dehydrogenation cycles. For commercial products activation should be as easy as possible in order to reduce the production cost of the hydride. Our proposition is that, by inducing strain and increasing the number of defects, severe plastic deformation techniques could be a way to improve the activation rate in magnesium-based alloys. We also studied the effect of cold rolling on hydrogen sorption properties of magnesium hydride. Similarly to ball milling, we expected that cold rolling could change the hydrogen sorption properties of magnesium hydrides.

EXPERIMENTAL

The magnesium used in this study was coming from a Norsk-Hydro ingot that was cut in small pieces. The magnesium plates were inserted between two Stainless Steel (316) plates of 0.8 mm thickness and rolled in air in a Durston DRM 100 modified in order to have the sample pass vertically through the rolls. This configuration enables easy processing of magnesium hydride powders. The apparatus' stainless steel rolls have a diameter of 6.5 cm and a length of 13 cm. Magnesium foils were rolled in air and after each roll, the foil was folded in two and rolled again thus giving a 50 % thickness reduction on each roll. The final thickness of the foil was 0.3 mm.

Magnesium hydride powder of 300 mesh and 98 % purity was provided by Alfa Aesar. New stainless steel plates were cleaned with alcohol prior to each experiment in order to protect our rolls and samples from cross-contamination. Cold rolling magnesium hydride powder consolidates the powder and changes its morphology to thin plates. The MgH_2 plate thicknesses varied from 0.3 to 0.8 mm. They were collected and rolled again to the desired number of rolling passes. Cold rolling under argon atmosphere was performed with the rolling machine inside a home-made glove box. From a light bulb method, the oxygen concentration inside the glove box was estimated to be 100 ppm and moisture level 1000 ppm [24]. A picture of the experimental set-up is shown in Fig. 1.

For microstructure characterization of the powders, we used a FEI Titan 80-300 (scanning) transmission electron microscope, equipped with a Gatan Image Filter (GIF) electron energy-loss spectrometer (EELS). A cryogenic holder was used in order to hinder *in situ* dehydrogenation. The STEM images were acquired using a high-angle annular dark-field (HAADF) detector. Low-loss EEL spectra were acquired at selected regions along with the HAADF signal (spectrum imaging). Characteristic plasmon excitation peaks of various phases (E_{Mg} = 10.6 eV, E_{MgH_2} = 14 eV, E_{MgO} = 21 eV) were used for mapping the location of each of the existing

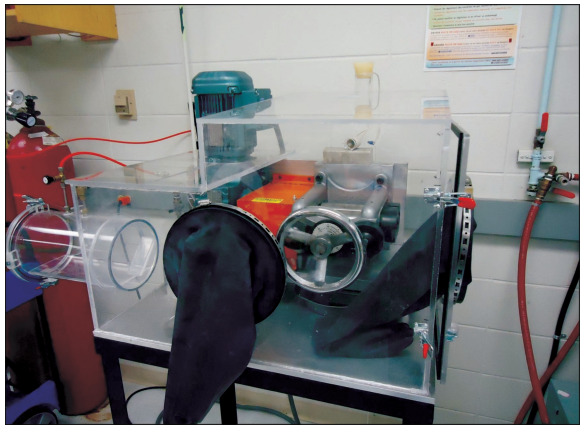

Fig. 1. Picture of the experimental set-up for cold rolling under argon.

phases. Complete description of the experimental technique used is given in reference [25].

Hydrogen absorption and desorption measurements were done on a homemade Sievert type PCT apparatus. Sample temperature was 623 K with a hydrogen pressure of 2 MPa in absorption and 0.06 MPa in desorption. The crystal structures were investigated by X-ray diffraction on a Bruker D8 Focus apparatus with Cu$K_{\alpha 1}$ radiation. The samples cold rolled under argon were measured by using a special sample holder that prevents air exposure. Crystallite size and microstrain were evaluated from Topas software [26] and using the volume weighted mean column height based on integral breath while micro strain was computed using broadening modelled by a Voigt function as recommended by Balzar *et al.* [27].

RESULTS AND DISCUSSION

Cold rolling of magnesium

Figure 2 shows the diffraction patterns of magnesium plates cold rolled 1, 5, 50, and 100 times in air compare to the as-received ingot. For easier comparison, just the three strongest peaks are shown. The ingot patterns shows the characteristics (100), (002) and (101) Bragg peaks. The peak position are shifted which indicates a change in lattice parameters. Figure 3 shows the variation of lattice parameters as a function of number of rolling passes. We see that the first rolling pass induces an important change of lattice parameters but the nominal values are recovered after 5 rolling passes. The reason for such important change after just one rolling pass is not understood at this moment. The other important change in the diffraction patterns is the relative intensities of the peaks. It is clear that after only one rolling pass a strong texture along (002) is induced. This texture changes only marginally with further rolling. Crystallite sizes and microstrains evaluated from Rietveld refinement are shown in Table 1. We see that the crystallite size actually increases after the first rolling. This surprising result is explained by the fact that the crystallite size evaluated from Rietveld refinement is the volume weighted mean column height of the particles. In the ingot sample the crystallites size is the average grains having all possible orientations. After one cold rolling pass, the crystallites are mainly oriented along (002) and thus what is effectively measured is the average volume of these oriented columns of Mg crystals.

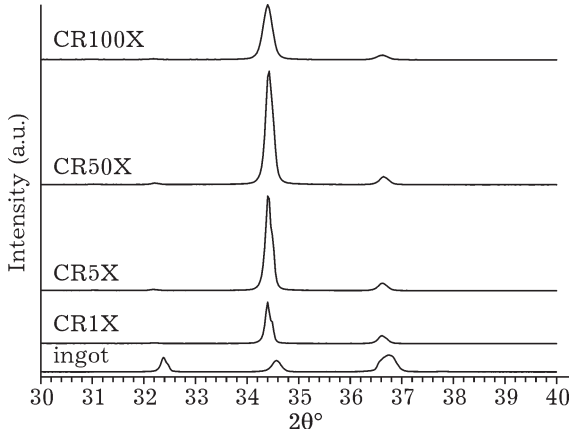

Fig. 2. X-ray diffraction patterns of magnesium as-received and cold rolled.

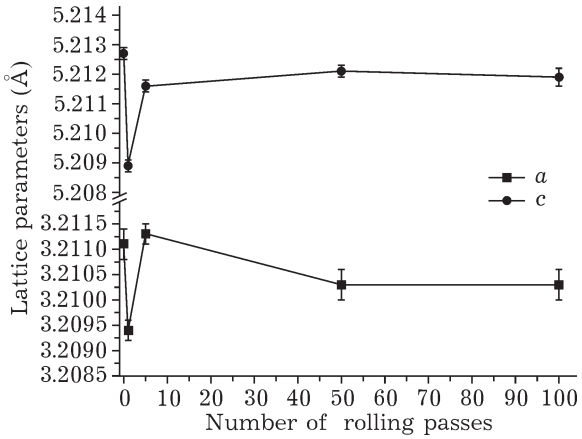

Fig. 3. Lattice parameters (*a* and *c*) of cold rolled magnesium.

TABLE 1

Crystallite size and microstrain of cold rolled magnesium

Samples	Crystallite size (nm)	Microstrain (%)
Ingot	113(3)	0.047(2)
CR1X	148(7)	0.049(8)
CR5X	150(5)	0.058(2)
CR50X	127(3)	0.068(1)
CR100X	89(3)	0.106(2)

Note. Number in parentheses is the uncertainty on the last significant digit.

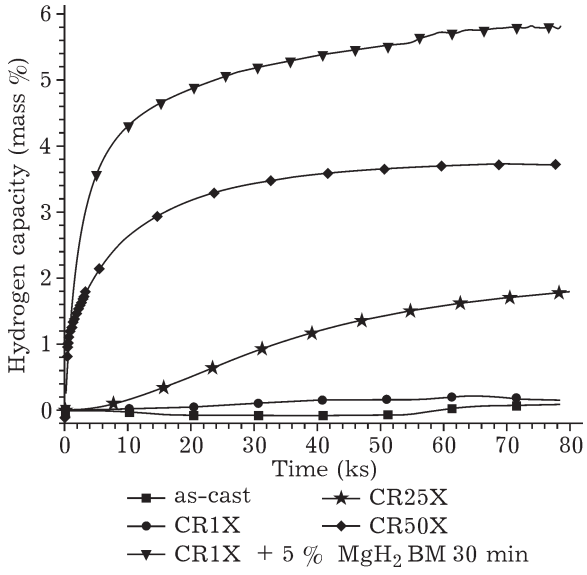

Fig. 4. First hydrogenation (activation) at 623 K under 2 MPa of hydrogen of; magnesium ingot as received, cold rolled one time, and cold rolled one time followed by a doping with 5 mass % MgH_2 by ball milling 30 min.

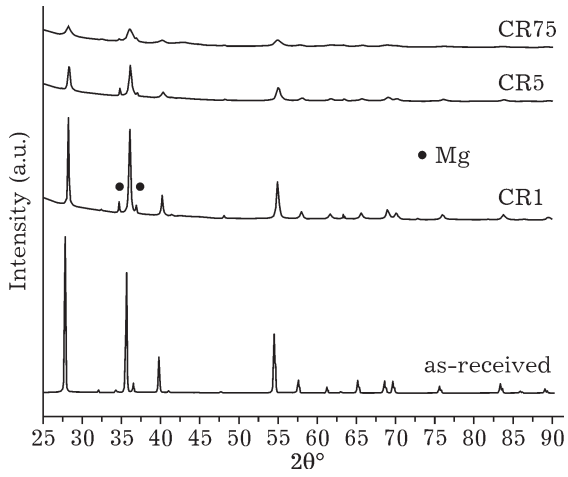

Fig. 5. X-ray diffraction patterns of magnesium hydride as-received and cold rolled in argon.

It is well known that the first hydrogenation of magnesium is very difficult. In order to get magnesium hydride, pure magnesium has to be exposed to high pressure of hydrogen at high temperature and for a long time. Activation at 623 K under 2 MPa of hydrogen of as-received magnesium as well as cold rolled 1, 25 and 50 times are shown in Fig. 3. It is clear that the as-received magnesium as well as cold rolled one time do not absorb hydrogen even after 80 000 s. As rolling number increases the activation is getting faster. This means that cold rolling has a positive effect on the activation behaviour. This could be explained by the decrease of crystallite size and the increases of defects as the number of rolling passes increases. However, such a high number of rolling pass-

TABLE 2

Crystallite size and microstrain of cold rolled MgH_2 in argon

Samples	Crystallite size (nm)	Microstrain (%)
As-received	116(2)	0.066(1)
CR1X	34.9(6)	0.067(4)
CR5X	17.1(3)	0.114(7)
CR75X	6.6(1)	0

Note. Number in parentheses is the uncertainty on the last significant digit.

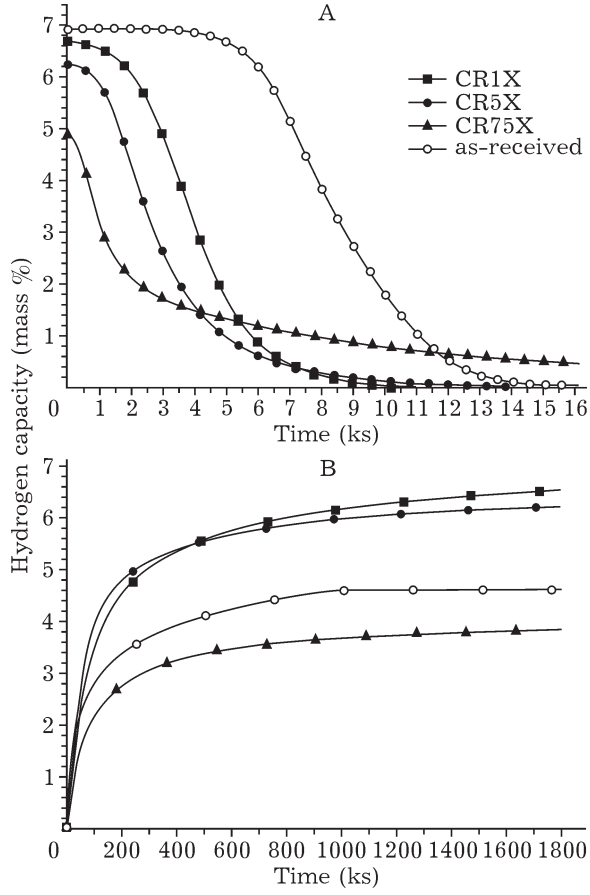

Fig. 6. Hydrogen sorption kinetics at 623 K of magnesium hydride cold rolled in argon: A – desorption under 0.06 MPa of hydrogen; B – absorption under 2 MPa of hydrogen.

es may not be practical for an industrial process. A potentially simpler method was recently shown [28]. In this method, the cold rolled magnesium is doped with 5 mass % of MgH_2 and the mixture is ball milled for 30 min. The sample then absorbs hydrogen very quickly and reaches a high hydrogen capacity as seen in Fig. 4.

Cold rolling of magnesium hydride

Usually, cold rolling is performed on metals or alloys. However, for hydrogen storage applications it may be interesting to directly cold roll the fully hydride material and study the effect on the hydrogen sorption behaviours,

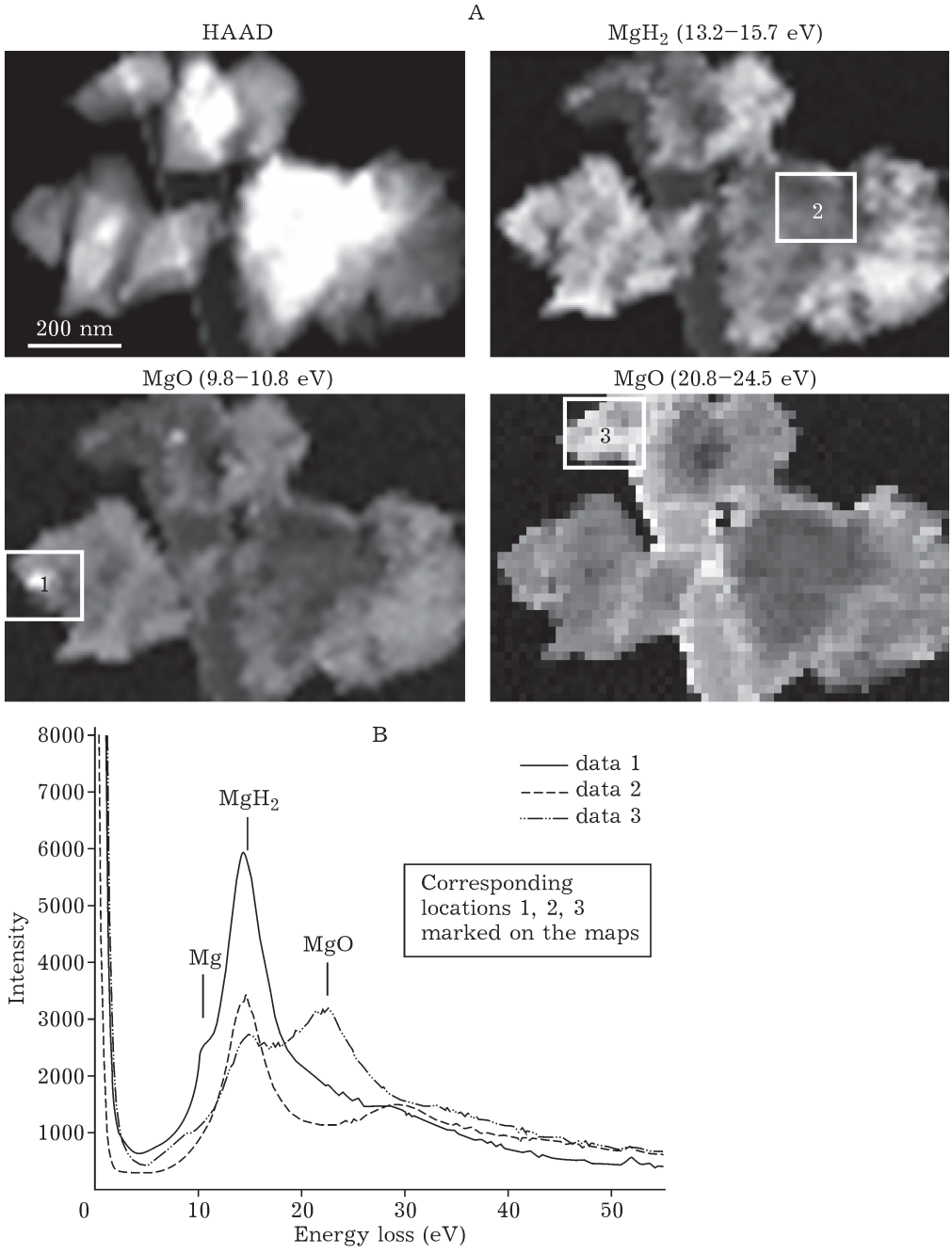

Fig. 7. (A) STEM-HAADF image of MgH_2 cold rolled in argon for 75 times along with energy-filtered maps corresponding to the various phases present. The energy range used for each map is given in the brackets. (B) EEL spectra from three locations, marked on the maps shown in (A).

especially sorption kinetics. The goal here is to see if cold rolling could replace ball milling as a way to obtain nanocrystalline structures in metal hydrides. As ball milling of magnesium hydride has been extensively studied, this hydride is a good candidate for this investigation.

Cold rolling in argon. Cold rolling of magnesium hydride was first performed in argon. Figure 5 shows the diffraction patterns of MgH_2 in the as-received state and rolled in argon atmosphere for 1, 2 and 75 times. The pattern of as-received material shows that there is a small amount of unreacted magnesium but all other peaks belong to the rutile type β-MgH_2. After only one roll the peaks are broadened which is an indication that the crystallite size is reduced. The pattern of the hydride rolled 5 times has broader peaks but also the relative intensities of the peaks are different. This means that a texture has been induced in the β-MgH_2. Moreover, close inspection of the pattern indicates that the remaining magnesium phase is also textured. Table 2 shows the crystallite sizes and microstrains as determined from Rietveld refinement. We see that cold rolling is very efficient to reduce crystallite size. The microstrain increases for the first few rolls but when the crystallites are very small then microstrain is essentially zero. The pattern of the sample rolled 75 times shows a broad peak associated to the presence of magnesium oxide. Even if the sample was processed in a glove box under argon after many rolling passes the materials is quite reactive and could easily be oxidized even under an atmosphere with low oxygen content. The hydrogen sorption kinetics of as-received and cold rolled in argon samples are shown in Fig. 6. The as-received sample presents a long incubation time in desorption. Cold rolling almost totally eliminates the incubation time and increases desorption kinetic. We see that just one cold rolling in argon drastically improves the sorption kinetics. Five rolling passes only marginally improves the sorption kinetics but the capacity is a little lower. Further rolling to 75 times greatly reduces the capacity due to the formation of magnesium oxide but even with the presence of oxide, the intrinsic desorption kinetic is faster than for the samples rolled one and five times. Thus, presence of a significant amount of oxide does not seem to reduce the sorption kinetics.

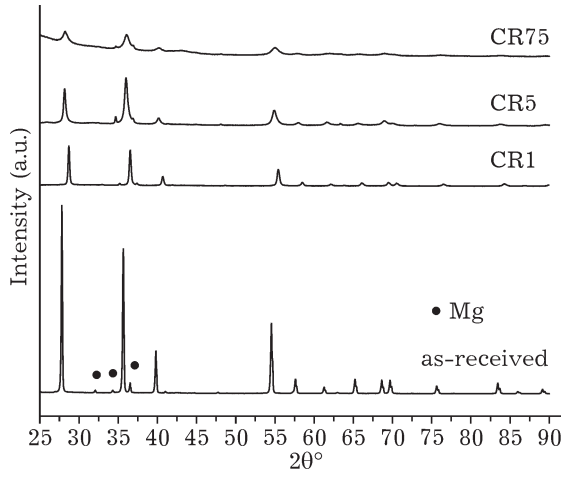

Fig. 8. X-ray diffraction patterns of magnesium hydride as-received and cold rolled in air.

In order to get a better knowledge of the microstructure of the rolled sample we performed TEM investigation. Figure 7A shows a STEM-HAADF image along with energy-filtered mappings of Mg, MgO and MgH_2 phases acquired by spectrum imaging (STEM/EELS) technique. These maps show that the particles are mainly MgH_2, with a small amount of Mg and a surface layer of MgO. Representative EEL spectra from the three locations of the sample is presented in Fig. 7B. Variation in brightness in the MgH_2 map is due to changes in thickness. This is a confirmation that even if the cold rolling was performed in argon atmosphere there is still formation of oxides and that these oxides are mainly on the surface of the particle.

Cold rolling in air. We have established that cold rolling magnesium hydride in argon improves the sorption kinetics but only for a few rolling passes. Performing cold rolling in protected atmosphere could be complicated and costly for industrial processes therefore we test-

TABLE 3

Crystallite size and microstrain of cold rolled MgH_2 in air

Samples	Crystallite size (nm)	Microstrain (%)
As-received	116(2)	0.066(1)
CR1X	49(1)	0.093(3)
CR5X	18.3(3)	0.184(5)
CR75X	6.6(1)	0

Note. Number in parentheses is the uncertainty on the last significant digit.

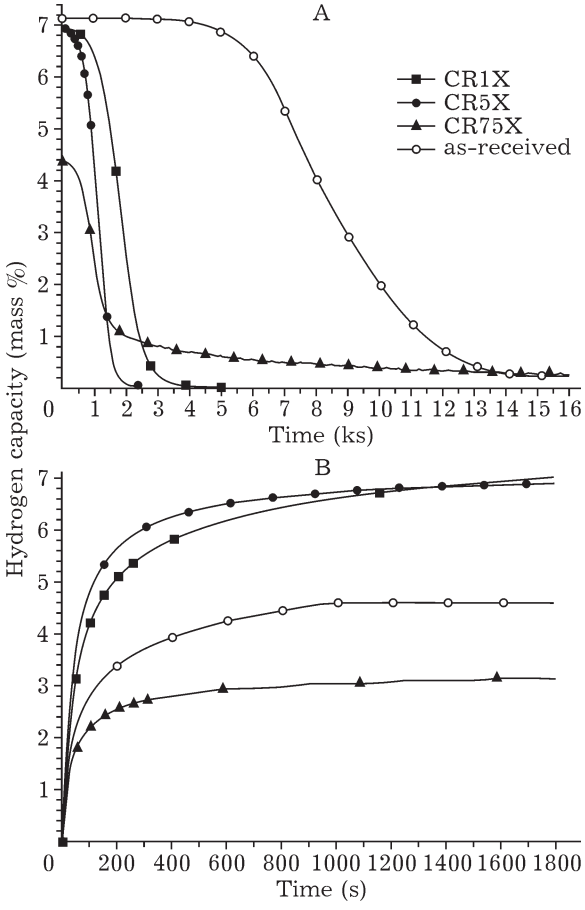

Fig. 9. Hydrogen sorption kinetics at 623 K of magnesium hydride cold rolled in air: A – desorption under 0.06 MPa of hydrogen; B – absorption under 2 MPa of hydrogen.

ed the effect of rolling in air. Figure 8 shows the diffraction patterns of MgH_2 rolled in air for 1, 2 and 75 times. The diffraction patterns are almost identical to the ones shown in Fig. 3. In fact, the crystallites sizes and microstrain deduced from Rietveld refinement and shown in Table 3 are essentially the same as the ones presented in Table 2. This could be expected because the rolling parameters were the same for the processes under air and argon.

Figure 9 shows the hydrogen absorption and desorption kinetics of magnesium hydride cold rolled in air. As in the case of rolling under argon atmosphere, the capacity decreases with the number of rolling. This is expected because rolling in air could easily produce oxides which will decrease the hydrogen capacity of the material. However, the surprising result is that, for each rolling number, the kinetics is faster than the corresponding material processed under argon. For small number of rolls the hydrogen capacity is only slightly reduced. When the number of rolls is high we see an important reduction of capacity.

CONCLUSIONS

In this investigation we showed that cold rolling of magnesium combined with a doping by MgH_2 by ball milling drastically reduces the first hydrogenation. However, for a better industrial process it would be preferable to perform all steps by cold rolling. We also showed that cold rolling of magnesium hydride is a good way to increase the hydrogen sorption kinetics as long as the number of rolling passes is limited. Rolling in air and in argon was performed and from a structural point of view both atmosphere produced similar materials. Even under protective atmosphere some oxidation takes place when the number of rolls is too large. The surprising result was that rolling in air is in fact better than rolling in argon in terms of hydrogen capacity and kinetics. The exact reason for this behaviour is still unknown and deeper investigation is needed.

Acknowledgements

N. Y. S., D. F. and J. H. would like to thanks the Ministry of Education of Perm Region (Russia) for funding project C-26/211. J. L., M. D., and J. H. would like to thanks the H2Can network for support. M. D would like to thank Prof. Gianluigi A. Botton for commenting on the microscopy results. The microscopy work was carried out at the Canadian Centre for Electron Microscopy, a facility supported by NSERC and McMaster University.

REFERENCES

1 Vegge T., Hedegaard-Jensen L. S., Bonde J., Munter T. R., Norskov J. K. // J. Alloys Compounds. 2005. Vol. 386. P. 1.
2 Sato T., Blomqvist H., Norйus D. // J. Alloys Compounds. 2003. Vol. 356–357. P. 494.
3 Song M.-Y. // Int. J. Hydrogen Energy. 1995. Vol. 20. P. 221.
4 Song M.-Y., Hong S.-H., Kwon I.-H., Kwon S.-N., Park C.-G., Bae J.-S. // J. Alloys Compounds. 2005. Vol. 398. P. 283.
5 Au M. // Mater. Sci. Eng. B. 2005. Vol. 117. P. 37.
6 Bellemare J., Huot J. // J. Alloys Compounds. 2012. Vol. 512. P. 33.
7 Vincent S. D., Huot J. // J. Alloys Compounds. 2011. Vol. 509. P. L175.
8 Leiva D. R., Floriano R., Huot J., Jorge A. M., Bolfarini C., Kiminami C. S., Ishikawa T. T., Botta W. J. // J. Alloys Compounds. 2011. Vol. 509. P. S444.

9 Lang J., Huot J. // J. Alloys Compounds. 2011. Vol. 509. P. L18.
10 Zhang L.T., Ito K., Vasudevan V. K., Yamaguchi M. // Acta Materialia. 2001. Vol. 49. P. 751.
11 Zhang L. T., Ito K., Vasudevan V. K., Yamaguchi M. // Mater. Sci. Eng. A. 2002. Vol. 329–331 P. 362.
12 Ueda T. T., Tsukahara M., Kamiya Y., Kikuchi S. // J. Alloys Compounds. 2004. Vol. 386. P. 253.
13 Dufour J., Huot J. // J. Alloys Compounds. 2007. Vol. 439. P. L5.
14 Dufour J., Huot J. // J. Alloys Compounds. 2007. Vol. 446–447. P. 147.
15 Huot J., Ravnsbćk D. B., Zhang J., Cuevas F., Latroche M., Jensen T. R. // Progress in Materials Science. 2013. Vol. 58. P. 30.
16 Leiva D. R., Costa H. C. A., Huot J., Pinheiro T. S., Jorge A. M., Ishikawa T. T., Botta W. J. // Mater. Res.-Ibero-Am. J. Mater. 2012. Vol. 15. P. 813.
17 Huot J., Skryabina N. Y., Fruchart D. // Metals. 2012. Vol. 2. P. 329.
18 Huot J. // Metals. 2012. Vol. 2. P. 22.
19 Amira S., Huot J. // J. Alloys Compounds. 2020. Vol. 520. P. 287.
20 Amira S., Santos S. F., Huot J. // Intermetallics. 2010. Vol. 18. P. 140.
21 Couillaud S., Enoki H., Amira S., Bobet J. L., Akiba E., Huot J. // J. Alloys Compounds. 2009. Vol. 484. P. 54.
22 Pedneault S., Roué L., Huot J. // Mater. Sci. Forum. 2008. Vol. 570. P. 33.
23 Pedneault S., Huot J., Roué L. // J. Power Sources. 2008. Vol. 185. P. 566.
24 Mao O., Altounian Z., StromOlsen J. O. // Rev. Sci. Instrum. 1997. Vol. 68. P. 2438.
25 Danaie M., Asselli A. A. C., Huot J., Botton G. A. // J. Phys. Chem. C. 2012. Vol. 116. P. 25701.
26 BRUKER_AXS Topas v4: General profile and structure analysis software for powder diffraction data, Karlsruhe, Germany, 2008.
27 Balzar D., Audebraund N., Daymond M. R., Fitch A., Hewat A., Langford J. I., Bail A. L., Louër D., Masson O., McCowan C. N., Popa N. C., Stephens P. W., Toby B. // J. Appl. Crystallogr. 2004. Vol. 37, P. 911.
28 Jain P., Lang J., Skryabina N. Y., Fruchart D., Santos S. F., Binder K., Klassen T., Huot J. // J. Alloys Compounds (in press).